Coherent states in a Rydberg atom: Quantum mechanics

Charles Cerjan,[1] Ernestine Lee,[2] David Farrelly,[2] and T. Uzer[3]
[1]*Lawrence Livermore National Laboratory, P.O. Box 808 M/S L-395, Livermore, California 94550*
[2]*Department of Chemistry and Biochemistry, Utah State University, Logan, Utah 84322-0300*
[3]*School of Physics, Georgia Institute of Technology, Atlanta, Georgia 30332-0430*
(Received 26 August 1996)

We present the quantal dynamics of electronic wave packets in the hydrogen atom in the presence of circularly polarized microwave and magnetic fields in regions of classical stability. Whereas wave packets may disperse without the stabilizing influence of a magnetic field, in its presence stable motion can be maintained for wave packets that are localized either at global equilibria that are either a maximum or minimum in a zero-velocity surface. Because these extrema are locally harmonic their vacuum states are truly coherent states in the original sense of Schrödinger. [S1050-2947(97)07303-4]

PACS number(s): 32.80.Rm, 05.45+b, 42.50.Hz

I. INTRODUCTION

Almost from that fateful day when wave mechanics destroyed the concept of an infinitely sharply localizable particle, physicists have been seeking paths from quantum to classical mechanics. Seventy years later, the quest continues. The Herculean task of reviewing the resulting literature is certainly beyond the scope of this publication: suffice it to say that one of the founding fathers of quantum mechanics, Schrödinger, was among the first to consider this daunting problem, and his thoughts on this matter are collected in his remarkably farsighted essay ''Der Uebergang von Mikro-zur Makromechanik'' (''The transition from microscopic to macroscopic mechanics'') [1], which, among other insights, anticipates the existence of ''scars,'' vestiges of classical mechanics in eigenstates [2]. Schrödinger's efforts were, however, not confined to philosophical speculation, since they resulted in the coherent states of the harmonic oscillator [3].

The concept of a coherent state can be summarized quite simply by following Schrödinger's own line of reasoning. Having found the stationary states of the harmonic oscillator, he realized that they could not represent a harmonically oscillating classical particle, being smeared out over the available position space. He proceeded to ask whether a superposition of these eigenstates could produce a wave packet that (i) suffered from minimal dispersion, (ii) evolved in time harmonically, and (iii) retained its minimal dispersion during this motion, just like a classical particle would. The well-known coherent states of the harmonic oscillator that he constructed represent the closest approximation, within the laws of quantum mechanics, to a classical particle and its motion under the influence of a Hooke's law force. In addition to being a striking illustration of the sought-after transition from quantum to classical mechanics, these states are also the mainstay of much of laser physics and quantum optics, mainly due to the pioneering efforts of Glauber [4].

Buoyed by his success, Schrödinger announced his discovery of the harmonic oscillator coherent states to Planck in a letter dated May 31, 1926 [5], and concluded: ''. . . I believe that it is only a question of computational skill to accomplish the same thing for the electron in a hydrogen atom.'' As before, he sought to superpose stationary states of the hydrogen atom into nondispersing wave packets that moved on the elliptic orbits generic to the Kepler-Coulomb problem, thereby creating as classical an atomic electron as quantum mechanics allows. Sadly, history shows that this optimistic expectation was never fulfilled. Before the end of the year, he wrote to Lorentz [5] that the ''. . . technical difficulties in the calculation were greater'' than in the harmonic oscillator case. The energy level structure of the hydrogen atom offers a revealing clue to his failure: In contrast to the harmonic oscillator spectrum, the energy levels of the hydrogen atom are not equally spaced and therefore the evolution frequencies of the eigenstates are not simply overtones of a fundamental frequency.

Schrödinger seems to have abandoned this problem, which then took its place among the arcana of mathematical physics. This publication is not the appropriate place to discuss the various group-theoretical arguments for and against the feasibility of constructing the coherent states of the bare Coulomb problem [6–18]. Instead, in this and the companion publication [19] we adopt a practical stance, namely, we search for the external field configurations that are likely to lead to new global equilibria in the effective potential since they may assist in localizing the electron in all three space dimensions especially if the effective potential is locally harmonic over a region large enough compared with the wavelength of the electron.

Recent advances in laser technology and Rydberg atom spectroscopy [20] have brought the classical limit of an atom within experimental reach mainly through the pioneering experiments of Yeazell and Stroud [21,14] and Stroud and coworkers [13,22–26]. In the process, classical concepts like orbits and turning points have enjoyed a revival [27]. Again, the literature of this field is much too extensive to review here and therefore, in the interest of space, we will merely summarize the findings of the last decade and then only when they concern our work: it is certainly possible, both theoretically and experimentally, to construct a wave packet that rides on an elliptic Kepler orbit [11,12] as well as circular orbits that correspond to maximal orbital angular momentum [28]. A common experimental strategy [29–33] is to work at very high quantum numbers, possibly (but not nec-

essarily) in the presence of an external electric field, to create regimes in which the local energy spacings are approximately constant. The electric field helps by splitting the states of a given principal quantum number manifold into equally spaced Stark states (to first order). Laser excitation is then used to form a spatially localized superposition of such atomic states [29]. However, while this wave packet can be localized in a plane and, within that plane, in the radial direction, it cannot be localized angularly. As a result it spreads along the elliptic orbit and interferes with itself, leading to experimentally detectable recurrences [27]. Empirically, the symmetry breaking due to multiple external fields must be used in order to achieve complete localization [30,31], but even under favorable circumstances, this triple localization (planar, radial, and angular) does not last very long—a brief encounter with the core is sufficient to undo it [30].

The close analogy between a Rydberg atom in a circularly polarized microwave field (CP) [34–38] and the restricted three-body problem (RTBP) [39] led us [40] and Bialynicki-Birula, Kalinski, and Eberly (BKE) [41] to discover independently that in the CP problem, stable equilibrium points exist that are analogous to the Lagrangian equilibrium points in celestial mechanics [39]. This analogy led BKE to expect that wave packets launched from the equilibrium points (analogs of the so-called Lagrange points L_4 and L_5) would orbit the nucleus without spreading. The Lagrange equilibrium points are stable maxima that support the Trojan asteroids of Jupiter, making the term ''Trojan'' wave packet appropriate for these states. However, the analogy between Rydberg atoms and planetary systems turns out to be fruitful but not perfect since the finite size of Planck's constant imposes an absolute scale on the atomic problem [42,43]. The atomic analogs of these points are stable only over a limited range of parameters, and placing a finite-size minimum uncertainty wave packet at such an equilibrium point becomes a delicate balancing act.

The announcement of the feasibility of nonstationary, nondispersive wave packets in the CP problem was greeted with a flurry of activity. For example, BKE showed that a curved wave packet [44] suffers very little, if any, of the dispersion that plagued their original wave packet because it nestles inside the effective potential of the CP field. Following the earlier discovery of similar Floquet states anchored to stable islands in the classical phase space of the linearly polarized microwave problem [45,46], Zakrzewski, Delande, and Buchleitner [47,48] have shown that it is possible to find eigenstates of the problem in a rotating frame that, being eigenstates, are immune to spreading. In the laboratory frame such eigenstates indeed orbit the nucleus without spreading. These states are neither wave packets nor coherent states in the sense of Schrödinger and will not mimic the harmonic oscillator coherent states; i.e., they are not minimum uncertainty wave packets since locally the equilibria in the CP problem are not harmonic [43]. Suggestions for the experimental preparation of these states can be found in the literature [48].

Our approach is substantially different and relies on manipulating the nature and stability of the equilibria by use of an additional magnetic field [42,49,50]. Classically we have shown that it is possible, using experimentally accessible fields, to create states that are extremely good approximations to the long sought for coherent states. Of course, as in the work of BKE these states are not free-atom states, being dressed now by the microwave and magnetic fields. Nevertheless, the classical simulations suggest that we now have the means to place an electron in a coherent state remote from the core.

Not only can the addition of a constant magnetic field perpendicular to the plane of polarization of the microwave field stabilize the localized states of this system but, more strikingly, a stable outer potential well can be created by using a slightly different field configuration [49,50]. This well is locally harmonic in a region of space that also excludes the nucleus, thereby allowing the wave packet to circle the nucleus safe from its detrimental influence on localization. Our prescription is most effective when the paramagnetic term is eliminated by a magnetic field, the Larmor procession of which compensates for the precession induced by the CP microwave field. Thereby, all velocity-dependent forces in the system are canceled and the equilibrium in question becomes a true potential minimum. Because it is locally harmonic to an excellent approximation, and indeed, both integrable and separable in elliptic coordinates [51,52], its vacuum state is a coherent state in the sense of Schrödinger to the same excellent approximation. The details of our prescriptions can be found in the companion paper [19] where modern methods of nonlinear dynamics are used to arrange the field configurations that support these states and to analyze their stability. The purpose of the present work is the fully quantum-mechanical investigation of these configurations. In particular, we demonstrate the superb accuracy of those classical predictions, which are based on the concept of a zero-velocity surface from celestial mechanics [39,42].

This paper is organized as follows: In Sec. II we give the Hamiltonian for the various field configurations and show their mapping onto the cranked oscillator, a well-known model in nuclear theory [53–56]. The computational details of the spectral grid method appear in Sec. III. Numerical results are presented in Sec. IV and a discussion of these results are presented in the last section.

II. HAMILTONIANS AND INITIAL WAVE FUNCTIONS

The Lagrangian for a hydrogen atom (in atomic units $a_0=\hbar=e=\mu=1$ and assuming an infinite nuclear mass) subjected simultaneously to a CP microwave field (field strength F and frequency ω_f) and a static magnetic field perpendicular to the plane of polarization of the CP field is

$$\mathcal{L}=\frac{\dot{x}^2+\dot{y}^2+\dot{z}^2}{2}+\frac{1}{r}-\frac{\pm\omega_c}{2}(x\dot{y}-y\dot{x}) \pm F(x\cos\omega_f t+y\sin\omega_f t), \tag{1}$$

where ω_c is the cyclotron frequency (sometimes denoted as the reduced magnetic field strength γ, where, $\gamma=B/2.35\times10^5$ T in atomic units) and the choice of sign is determined by the direction of the magnetic field in the case of the paramagnetic term. The sign of F is immaterial but our convention, consistent with the companion paper [19], is to choose this sign such that global equilibria corresponding to maxima or minima will turn out to lie along the positive x

axis (note that this convention differs from the one used by BKE). The time dependence in Eq. (1) may be eliminated by going to a frame that rotates at the constant angular velocity ω_f, which finally leads to the Hamiltonian

$$H=K=\frac{p_x^2+p_y^2+p_z^2}{2}-\frac{1}{r}-\omega(xp_y-yp_x)\mp Fx + \frac{\omega_c^2}{8}(x^2+y^2). \tag{2}$$

where K is analogous to the Jacobi constant in the RTBP [39] and $\omega=(\omega_f\mp\omega_c/2)$. As was explained in the companion paper [19], when the Hamiltonian contains a nonconserved paramagnetic term, a type of potential—in the language of celestial mechanics, i.e., a zero-velocity surface (ZVS)—can be constructed and provides an excellent guide to the dynamics [39]. The ZVS is given by rewriting the Hamiltonian in terms of velocities instead of momenta and is

$$V=H-\frac{\dot{x}^2+\dot{y}^2+\dot{z}^2}{2}=-\frac{1}{r}\mp Fx-\frac{\omega_f(\omega_f\mp\omega_c)}{2}(x^2+y^2). \tag{3}$$

The equilibria that result from the two possible signs in the coefficient of the paramagnetic term and their stability form a major ingredient of the companion publication [19]. Therefore, for conciseness x_0 is used to refer simply to an equilibrium point.

While the most common situation in atomic physics is stable motion at a potential energy minimum the problem in hand does not meet this criterion because of the presence of the paramagnetic term; i.e., one cannot identify separate kinetic and potential parts of the Hamiltonian. A key point of our configuration of fields is the latitude it provides to vary or even eliminate the paramagnetic term. When it is allowed to be present, the paramagnetic term complicates the computation of the frequencies associated with the coherent state since there is no ''potential'' about which to expand. However, for both the maximum and the minimum configurations the strategy to be described is used to compute frequencies of the initial coherent state. The steps involved are (a) a transformation to a barycentric system of Cartesian coordinates at the equilibrium, (b) expansion of the ZVS in a power series to second order—this produces what is known in nuclear physics as a *cranked oscillator*, which is separable and harmonic at once, albeit in rotated coordinates, (c) determination of the locally harmonic frequencies of these oscillators, and (d) computation of the vacuum state of the cranked oscillator. For future reference, we will give the derivation of the initial wave packet in some detail since phase factors are essential in obtaining fully coherent wave packets.

A. Relation to the restricted three-body problem

We will begin by relating the atomic Hamiltonians described above to the RTBP, the canonical form of which is given by [39,57,58]

$$H=\frac{1}{2}(p_x^2+p_y^2)-(xp_y-yp_x)-\frac{1-\mu}{\rho_1}-\frac{\mu}{\rho_2}, \tag{4}$$

with μ being the mass ratio and

$$\rho_1=\sqrt{(x+\mu)^2+y^2},\quad \rho_2=\sqrt{(x+\mu-1)^2+y^2},\quad \gamma=1-2\mu. \tag{5}$$

The stability of motion at the equilibria is solved generally by shifting the origin of the initial coordinate system based on the center of mass to another, synodical coordinate system centered around the Lagrangian point L_4 given by

$$x=\frac{1}{2}\gamma,\quad y=\frac{\sqrt{3}}{2},\quad p_x=\frac{\sqrt{3}}{2},\quad p_y=-\gamma/2 \tag{6}$$

by the conservative, completely canonical diffeomorphism

$$x=\frac{1}{2}\gamma+\xi,\quad p_x=\frac{\sqrt{3}}{2}+p_\xi,\quad y=\frac{\sqrt{3}}{2}+\eta,\quad p_y=-\frac{1}{2}\gamma+p_\eta. \tag{7}$$

The RTBP Hamiltonian is thereby converted to

$$H=\tfrac{1}{2}(p_\xi^2+p_\eta^2)-(\xi p_\eta-\eta p_\xi)-\Omega, \tag{8}$$

where

$$\Omega=\frac{1}{2}\gamma\xi+\frac{\sqrt{3}}{2}\eta+\frac{1}{2}\left(\frac{1+\gamma}{\rho_1}+\frac{1-\gamma}{\rho_2}\right). \tag{9}$$

When this last quantity is expanded around the equilibrium point, a cranked oscillator is obtained.

B. Mapping onto the cranked oscillator

The Hamiltonian (8) is similar to the cranked anisotropic oscillator model that has been used in nuclear physics to generate basis vectors for self-consistent calculations to model collective rotations [53–56]. The derivation of a similar cranked oscillator, albeit in three dimensions, was outlined in the companion paper. The mapping begins with the expansion of the ZVS around the equilibrium point corresponding to a maximum, $L_{\max}$: The transformation from the original rotating (synodic) center of mass coordinates to the equilibrium configuration L_b is accomplished through the canonical transformation

$$x=x_0+\xi,\quad p_x=p_\xi,\quad y=\eta,\quad p_y=\omega x_0+p_\eta,\quad z=\zeta,\quad p_z=p_\zeta, \tag{10}$$

which transforms the Hamiltonian (2) into the form

$$H=\frac{p_\xi^2+p_\eta^2+p_\zeta^2}{2}-\omega(\xi p_\eta-\eta p_\xi)+\Theta. \tag{11}$$

where the ''force function'' [57] is given by

$$\Theta = -\frac{1}{r} \mp F\left(\xi + x_0 + \frac{\omega_c^2}{8}(\xi^2+\eta^2) - \frac{1}{2}\omega^2 x_0^2 + \frac{1}{8}\omega_c^2 x_0^2 + \left(\frac{\omega_c^2}{4} - \omega^2\right) x_0 \xi, \right. \tag{12}$$

which may be expanded around $(\xi,\eta,\zeta)=(0,0,0)$ to produce an approximate Hamiltonian describing librations around L_b,

$$\mathcal{H} = H + H_c,$$

where

$$H = \frac{p_\xi^2 + p_\eta^2 + p_\zeta^2}{2} + \frac{\omega^2}{2}(a\xi^2 + b\eta^2 + c\zeta^2) - \omega(\xi p_\eta - \eta p_\xi) + H_c, \tag{13}$$

with

$$a = \frac{1}{\omega^2}\left(\frac{\omega_c^2}{4} - \frac{2}{x_0^3}\right), \quad b = \frac{1}{\omega^2}\left(\frac{\omega_c^2}{4} + \frac{1}{x_0^3}\right), \quad c = \frac{1}{\omega^2 x_0^3}, \tag{14}$$

and the part of the Hamiltonian containing only constant terms is given by

$$H_c = -\frac{1}{2}\omega^2 x_0^2 \mp F x_0 + \frac{1}{8}\omega_c^2 x_0^2 - \frac{1}{x_0}. \tag{15}$$

From Cauchy's uniqueness theorem it follows that a particle starting out in the plane of polarization, with an initial velocity contained in that plane, will never leave the plane [59]. The linear stability at the equilibrium point (for both the maximum and minimum) was derived in detail in the companion paper [19]. Briefly, the approximation to the Hamiltonian describing librations around the equilibrium point shows the motion in the z (or ζ) direction to be stable, harmonic, and decoupled from the planar motion. Therefore, for initial conditions in the $\xi\eta$ plane, the motion can be treated as being restricted to that plane. Rewriting this operator in the plane $\zeta=0$ reduces it to the two-dimensional form used in our numerical calculations.

After a rotation in phase space (described in detail in Refs. [53–56])

$$\begin{aligned} \xi' &= A\xi + Bp_\eta, \\ \eta' &= A\eta + Bp_\xi, \\ p'_\xi &= p_\xi + C\eta, \\ p'_\eta &= p_\eta + C\xi, \end{aligned} \tag{16}$$

with $A - BC = 1$ (to preserve the commutation relations between coordinates and momenta) H can be reduced to the following separable form [55]:

$$H = \frac{1}{2m_\xi} p'^2_\xi + \frac{1}{2} m_\xi \Omega_\xi^2 \xi'^2 + \frac{1}{2m_\eta} p'^2_\eta + \frac{1}{2} m_\eta \Omega_\eta^2 \eta'^2, \tag{17}$$

where

$$m_\xi = \frac{\Omega_\xi^2 - \Omega_\eta^2}{\Omega_\xi^2 - a\omega^2 + \omega^2}$$

and

$$m_\eta = \frac{\Omega_\eta^2 - \Omega_\xi^2}{\Omega_\eta^2 - b\omega^2 + \omega^2}. \tag{18}$$

The locally harmonic frequencies are given by

$$\Omega_\eta^2 = \tfrac{1}{2}(\omega_\xi^2 + \omega_\eta^2) + \omega^2 - \tfrac{1}{2}S, \tag{19}$$

$$\Omega_\xi^2 = \tfrac{1}{2}(\omega_\xi^2 + \omega_\eta^2) + \omega^2 + \tfrac{1}{2}S, \tag{20}$$

where

$$S = \mathrm{sgn}(\omega_\eta - \omega_\xi)\sqrt{(\omega_\xi^2 - \omega_\eta^2)^2 + 8\omega^2(\omega_\xi^2 + \omega_\eta^2)}, \tag{21}$$

with $\omega_\xi = |\omega|\sqrt{a}$, $\omega_\eta = |\omega|\sqrt{b}$, and $\omega_\zeta = |\omega|\sqrt{c}$.

In what follows, we will assume that $\omega_\eta > \omega_\xi$. However, the needed changes are obvious if this is not the case. The cranked oscillator has not been explicitly derived for the case of inclusion of a magnetic field before and, therefore, we give the expressions for the frequencies explicitly in terms of the dimensionless quantities

$$q = \frac{1}{\omega^2 x_0^3}, \tag{22}$$

$$\omega_s = \omega_c / \omega. \tag{23}$$

The auxiliary quantity S becomes

$$S = \omega^2\sqrt{9q^2 - 8q + 4\omega_s^2}, \tag{24}$$

which turns the locally harmonic frequencies into

$$\Omega_\eta^2 = \omega^2\left(\tfrac{1}{4}\omega_s^2 + 1 - \tfrac{1}{2}q - \tfrac{1}{2}\sqrt{9q^2 - 8q + 4\omega_s^2}\right), \tag{25}$$

$$\Omega_\xi^2 = \omega^2\left(\tfrac{1}{4}\omega_s^2 + 1 - \tfrac{1}{2}q + \tfrac{1}{2}\sqrt{9q^2 - 8q + 4\omega_s^2}\right) \tag{26}$$

and the masses into

$$m_\xi = \frac{\sqrt{9q^2 - 8q + 4\omega_s^2}}{(2 + \tfrac{3}{2}q) + \tfrac{1}{2}\sqrt{9q^2 - 8q + 4\omega_s^2}} \tag{27}$$

and

$$m_\eta = \frac{-\sqrt{9q^2 - 8q + 4\omega_s^2}}{(2 - \tfrac{3}{2}q) - \tfrac{1}{2}\sqrt{9q^2 - 8q + 4\omega_s^2}}. \tag{28}$$

The resulting masses may be positive or negative. There is no bound motion if both masses are negative. In the case of motion at a maximum, the masses have opposite signs. Based on the zero-velocity surface, this case occurs when $\omega^2 > \omega_\xi^2, \omega_\eta^2$. When both masses are positive, stable motion at a minimum is indicated. In order to cover the two possibilities for stable motion, we define the index

$$\Lambda = \frac{m_\xi m_\eta}{|m_\xi m_\eta|}, \tag{29}$$

which is 1 for a minimum and -1 for a maximum.

The energy eigenvalues are given by

$$E = \frac{m_\xi}{|m_\xi|}\left(n_\xi + \frac{1}{2}\right)\hbar|\Omega_\xi| + \frac{m_\eta}{|m_\eta|}\left(n_\eta + \frac{1}{2}\right)\hbar|\Omega_\eta|. \tag{30}$$

The magnitude of the ground-state energy is defined in terms of an average frequency Ω through

$$E = \frac{\hbar}{2}\left(|\Omega_\xi| + \Lambda|\Omega_\eta|\right) = \hbar\Omega \tag{31}$$

with this frequency explicitly given by

$$\Omega = \frac{|\omega|}{2}\sqrt{2 - q + \tfrac{1}{2}\omega_s^2 + 2\Lambda s(q,\omega_s)}, \tag{32}$$

where

$$s(q,\omega_s) = \sqrt{(1 + 2q - \tfrac{1}{4}\omega_s^2)(1 - q - \tfrac{1}{4}\omega_s^2)}. \tag{33}$$

C. The initial wave packet

We express the ground-state wave function of our three-dimensional electronic Hamiltonian as

$$\Psi_{000}(\xi,\eta,\zeta) = N\psi_C(\xi,\eta)\exp\left(-\frac{\omega_\zeta}{2}\zeta^2\right), \tag{34}$$

where $\psi_C(\xi,\eta)$ is the normalized ground-state wave function of the cranked oscillator and is given by

$$\psi_C(\xi,\eta) = \left(\frac{\alpha\beta}{\pi^2}\right)^{1/4}\exp\left(-\frac{\alpha}{2}\xi^2 - \frac{\beta}{2}\eta^2 - i\gamma\xi\eta\right). \tag{35}$$

In order to determine the parameters α,β,γ the quantity Q is needed:

$$Q = \frac{(a-b)\omega^2}{4(\Omega^2 - \omega^2)}, \tag{36}$$

which is explicitly

$$Q = \frac{2 + q + 2\Lambda s(q,\omega_s) - \frac{1}{2}\omega_s^2}{3q}. \tag{37}$$

The parameters α,β,γ are given by

$$\alpha = \Omega(1+Q)/\hbar, \tag{38}$$

i.e.,

$$\alpha = \left(\frac{\omega}{3q\hbar}\right)(1 + 2q - \tfrac{1}{4}\omega_s^2 + \Lambda s)\sqrt{2 - q + \tfrac{1}{2}\omega_s^2 + 2\Lambda s(q,\omega_s)}, \tag{39}$$

$$\beta = \Omega(1-Q)/\hbar, \tag{40}$$

i.e.,

$$\beta = \left(\frac{\omega}{3q\hbar}\right)(q - 1 + \tfrac{1}{4}\omega_s^2 - \Lambda s)\sqrt{2 - q + \tfrac{1}{2}\omega_s^2 + 2\Lambda s(q,\omega_s)}, \tag{41}$$

$$\gamma = \omega Q/\hbar, \tag{42}$$

i.e.,

$$\gamma = \left(\frac{\omega}{3q\hbar}\right)(2 + q - \tfrac{1}{2}\omega_s^2 + 2\Lambda s). \tag{43}$$

When the stabilizing magnetic field is absent ($\omega_s = 0$), these parameters reduce to the ones used by BKE [41] (after interchanging x and y and reversing the sign of ω to account for differences in our conventions.)

D. Phase factors

The transformation to barycentric synodical coordinates requires two shifts, one in coordinate and another in momentum, to reach the equilibrium point from the center of mass. The quantum mechanical consequence of these shifts can be described by a translation operator

$$\mathcal{T}(x_0) = \exp(-ix_0 p_\xi/\hbar) \tag{44}$$

and a boost operator

$$\mathcal{B}(\omega x_0) = \exp(i\omega x_0\,\eta/\hbar). \tag{45}$$

If $|C\rangle$ is the ket that is represented by $\psi_C(\xi,\eta)$, then the ket $|I\rangle$ that we need to use as the initial state in the barycentric coordinates is related to it by

$$|I\rangle = \mathcal{T}(x_0)\mathcal{B}(\omega x_0)|C\rangle \tag{46}$$

and therefore the wave functions are related by

$$\psi_C(x,y) = \left(\frac{\alpha\beta}{\pi^2}\right)^{1/4}\exp(i\nu x_0 y)\exp\left[-\frac{\alpha}{2}(x - x_0)^2 - \frac{\beta}{2}y^2 - i\gamma(x - x_0)y\right], \tag{47}$$

where $\nu = \omega/\hbar$.

In the simulations that follow, the procedure described above was used to generate a coherent state, either classically or quantum mechanically, as given by Eq. (47). The same procedure is valid both at the maximum and at the minimum.

III. COMPUTATIONAL DETAILS

It is convenient for numerical manipulations to scale the spatial coordinates by the square root of the frequency, $x \to x'/\sqrt{\omega_c}$ and $y \to y'/\sqrt{\omega_c}$. This scaling produces the operator (we have dropped the primes for convenience)

$$H = \frac{1}{2}(p_x^2 + p_y^2) - \frac{1}{\sqrt{\omega_c}\sqrt{x^2+y^2}} - \left(\frac{\omega_f}{\omega_c} \pm \frac{1}{2}\right)(xp_y - yp_x) \mp \frac{Fx}{\omega_c^{3/2}} + \frac{(x^2+y^2)}{8}, \tag{48}$$

where the energy is in units of ω_c and the time in units of inverse frequency. For the case of no magnetic field discussed below, the analogous scaling may be applied using ω_f in place of the cyclotron frequency so that the operator becomes

$$H=\frac{1}{2}(p_x^2+p_y^2)-\frac{1}{\sqrt{\omega_f}\sqrt{x^2+y^2}}-(xp_y-yp_x)+\frac{Fx}{\omega_f^{3/2}}. \tag{49}$$

The time-independent Schrödinger equation was solved for these two-dimensional operators by applying a pseudospectral grid method for the spatial representation of the derivatives and a Chebyshev time advancement algorithm [60]. The initial wave packet was selected as in Eq. (47) with the factor ν chosen to be $(\omega_f/\omega_c \pm 0.5)$ for a nonzero magnetic field and 1 otherwise. This time-independent initialization was adopted on the basis of the zero-velocity surface initial conditions needed to maintain localization of the classical trajectories [40]. Numerical stability was checked by grid parameter variation for all cases. It was found that grids of 256×256 were sufficient for the magnetic field cases. Numerical contamination was always present in the zero magnetic field calculations, probably due to the unbounded nature of the potential, so larger grids of 512×512 were used to verify the results, although we do not present our comparisons with the BKE results [41]. The numerical procedure was also validated by comparing to the exact results known for the cranked oscillator system.

We present our results as a progression from somewhat dispersive cases to the culmination of our efforts, namely, a coherent state in the sense of Schrödinger. The choice of the physically relevant parameters follows from previous classical [42] and quantal propagation studies [49]. Case 1 corresponds to classically stable behavior at a maximum of the zero-velocity surface. Then, reversing the direction of the magnetic field, we arrive at case 2: There, the initial conditions are selected at a minimum of the zero-velocity surface where the frequencies due to the CP and external magnetic fields are opposed but do not cancel the paramagnetic term. In such a case, our calculations show that the dynamics at the higher energies inside the well are chaotic [50]. Finally, in case 3, the paramagnetic term is canceled and the initial wave packet circles the nucleus without dispersion: a true coherent state.

We use two measures to diagnose quantum-mechanical state localization. One is the autocorrelation function, which is defined as

$$\sigma_a(t)=\int_{-\infty}^{\infty}\psi^*(x,y,t)_{\rm init}\psi(x,y,t)dx\ dy, \tag{50}$$

where $\psi(x,y,t)_{\rm init}$ is the initial wave packet. Another possible measure of the deviation from stationary behavior is the time dependence of the virial commutator,

$$\sigma_v(t)=\int_{-\infty}^{\infty}\psi^*(x,y,t)[H(x,y),p_xx+p_yy]\psi(x,y,t)dx\ dy. \tag{51}$$

The classical virial theorem states that if the motion is damped or periodic then the time average of the virial expression establishes a relation between the kinetic and potential energy contributions [61]. The quantal analog is provided by the Heisenberg equations of motion. As is well known, if a stationary state is used for the averaging then the virial expression vanishes, again providing a relation between the different energy contributions. For the specific case of the Hamiltonian operators above, the commutator of the virial operator, p_xx+p_yy, with the Hamiltonian operator, produces

$$[H,p_xx+p_yy]=(p_x^2+p_y^2)-V(x-x_0). \tag{52}$$

Thus if the expectation value of the right-hand side is constant or periodic, the quantal motion is localized.

IV. RESULTS

The results of the calculations are summarized in Figs. 1–3. The first set of figures corresponds to case 1, where the initial wave packet is placed at a maximum of the ZVS, which has been ''flattened'' with an external magnetic field [42]. The time is in units of ω_c with a total time of 12 field cycles for this calculation and corresponds to 362 ps. This is a somewhat counterintuitive arrangement for those who are used to thinking of stable motions as being confined to minima of a potential. But as argued before, the initial phase conditions ensure that the centrifugal terms will dominate, effectively preventing the transfer of potential to kinetic energy. The autocorrelation function is highly periodic and regular. Thus this case mimics the highly localized behavior of case 2 below. For the present conditions this time dependence is nearly periodic with no perceptible growth over the 12 cycle propagation time.

Reversing the direction of the magnetic field brings us to case 2. The wave packet is placed at the outer minimum but is subject to a nonconserved paramagnetic term. The duration of the integration is again 12 cycles, which, because of the higher value of ω_c is 106 ps. The time dependence of the absolute value of the autocorrelation function is plotted in Fig. 2(a) and is seen to be regular and highly periodic. In spite of the detrimental effect of the paramagnetic term, the initial wave packet clearly remains highly localized. The amplitude of the initial wave packet is plotted in Fig. 2(b), with the contour representation in Fig. 2(c). The final wave packet is plotted analogously in Figs. 2(d) and 2(e). Inspection of these figures corroborates the highly correlated nature of the propagation. On the other hand, a plot of the virial commutator time dependence, presented in Fig. 2(f), reveals a slow but perceptible growth, which is an indication of a slow loss of correlation.

Case 3 represents the culmination of our efforts. The Larmor precession due to the external magnetic field and the precession due to the CP field cancel the paramagnetic term exactly. The result is an integrable system with an outer minimum, well away from the nucleus, which is locally harmonic [49,50]. Consequently, its vacuum state is coherent

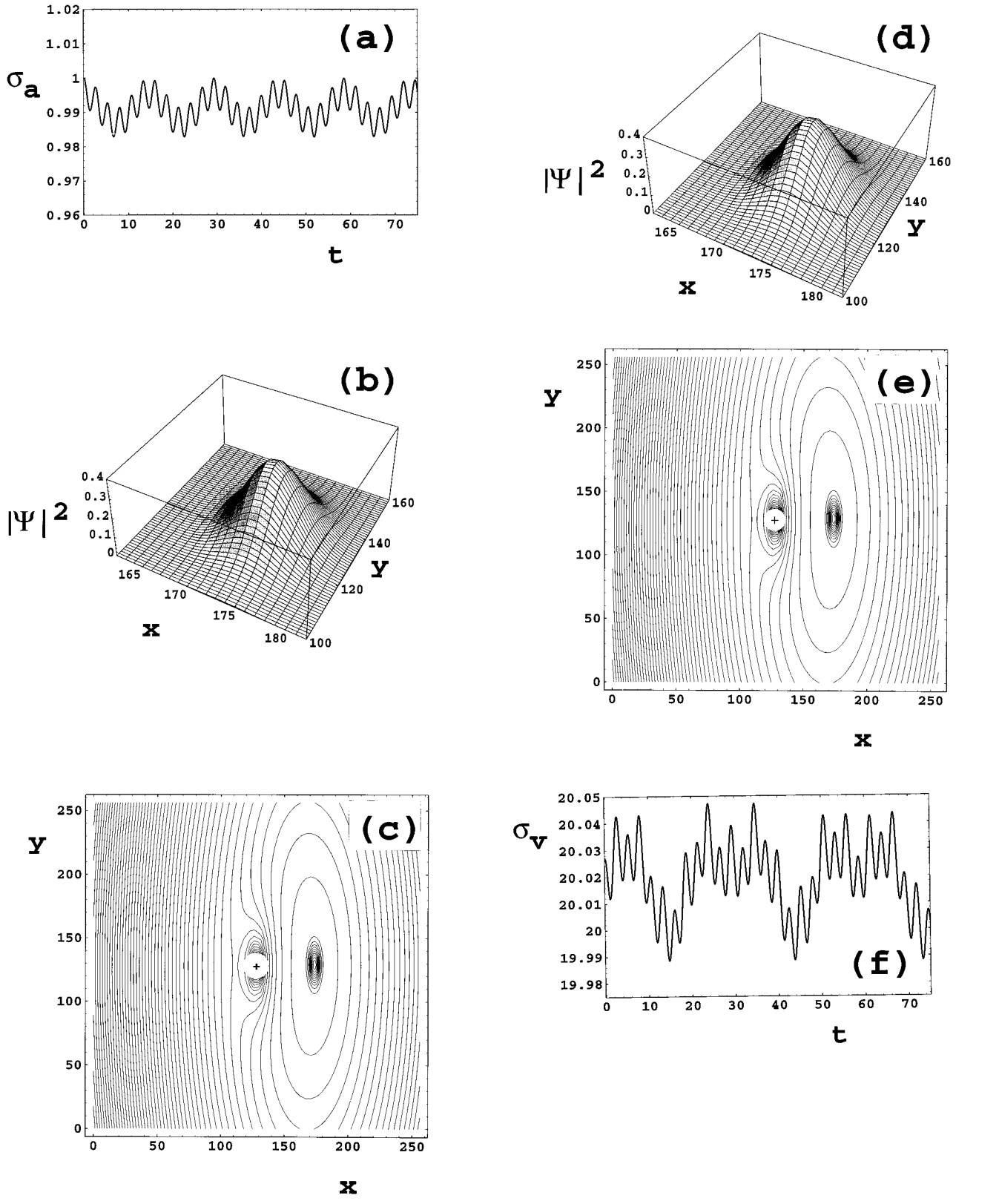

FIG. 1. Quantum evolution of a wave packet initially placed at a *maximum*. The parameters in Eq. (2) are, in atomic units, $F=5.000(-8)$, $\omega_c=5.000(-6)$, $\omega_f=1.000(-6)$. The maximum L_m is at $x_0=10\,000.0$. The parameters for the wave packet given in Eq. (47) are as follows: $\alpha=2.698\,74(-6)$, $\beta=2.133\,54(-6)$, $\gamma=4.09371(-7)$. The plots are in the scaled units of Eq. (48) and the nucleus is shown by the symbol $\oplus$. (a) Autocorrelation function as a function of time, Eq. (50). (b) Wave packet ($|\Psi|^2$) at time $t=0$ on a section of the 256×256 grid used in the fast Fourier transform (FFT) calculations [x range=(−64, 64) scaled units and the y range is (−19, 19) scaled units]. (c) Contour diagram of wave packet at $t=0$ on the FFT grid. Also shown is a contour plot of the ZVS [Eq. (3)], (d) wave packet at the end of 12 cycles. (e) Contour diagram of the wave packet at $t=12$ cycles. (f) Time dependence of the virial commutator, Eq. (51).

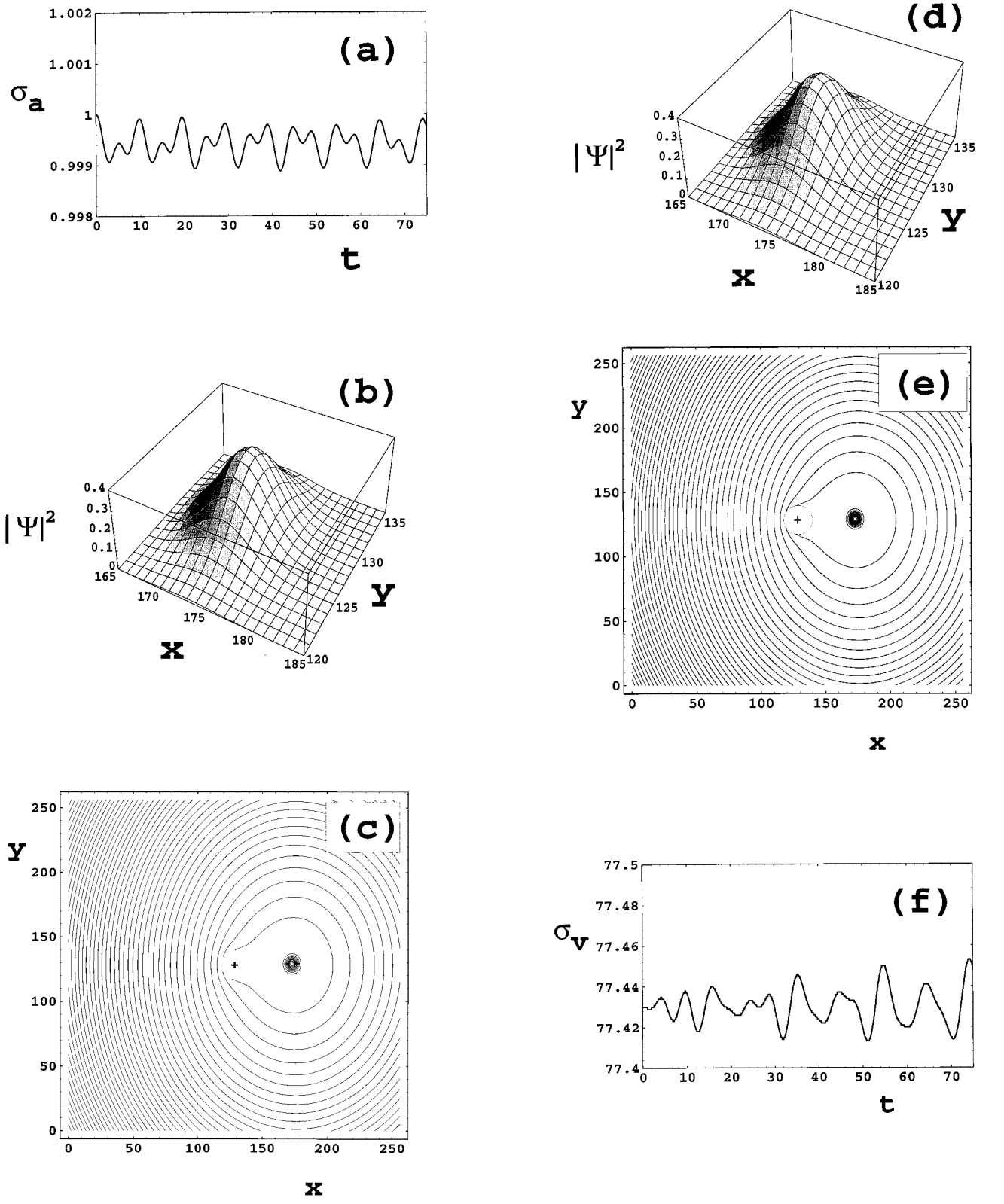

FIG. 2. Quantum evolution of a wave packet initially placed at a *minimum* with nonvanishing paramagnetic term. The parameters in Eq. (2) are, in atomic units, $F=3.8997(-7)$, $\omega_c=1.705\,59(-5)$, $\omega_f=6.037\,78(-6)$. The minimum L_m is at $x_0=5332.28$. The parameters for the wave packet given in Eq. (47) are as follows: $\alpha=7.654\,84(-6)$, $\beta=8.963\,06(-6)$, $\gamma=1.960\,33(-7)$. Units and definitions as in Fig. 1. (a) Autocorrelation function as a function of time, Eq. (50). (b) Wave packet at time $t=0$ on a section of the 256×256 grid used in the FFT calculations [x range$=(-64, 64)$ scaled units and the y range is $(-52, 52)$ scaled units]. (c) Contour diagram of wave packet at $t=0$. (d) Wave packet at the end of 12 cycles. (e) Contour diagram of the wave packet at $t=12$ cycles. (f) Time dependence of the virial commutator, Eq. (51).

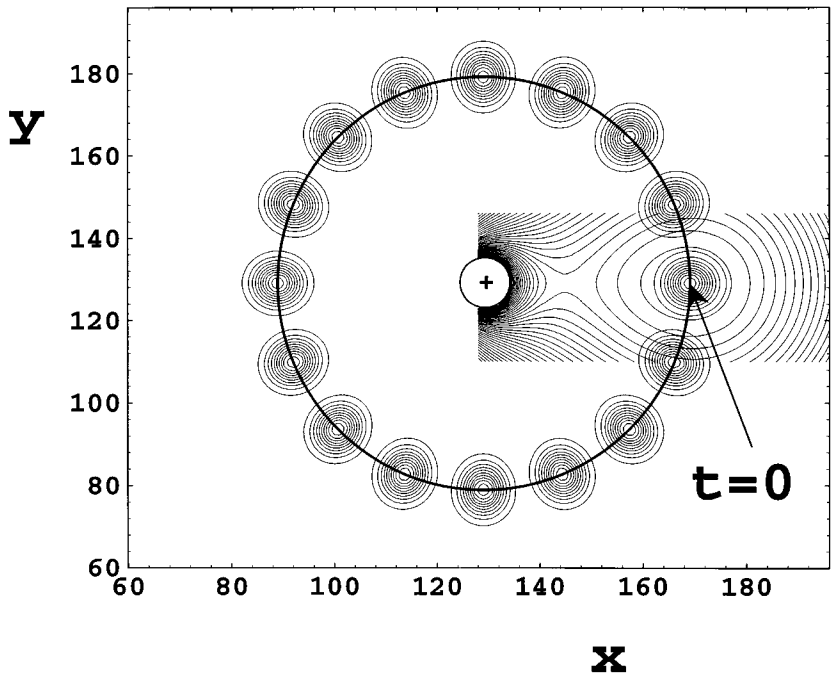

FIG. 3. Quantum evolution of a wave packet initially placed at a minimum with vanishing paramagnetic term. This is an excellent approximation to a rigorously coherent state. The parameters in Eq. (2) are, in atomic units: $F=3.899(-7)$, $\omega_c=1.6887(-5)$, $\omega_f=8.4435(-6)$. The minimum L_m is at $x_0=4880.0$. The parameters for the wave packet given in Eq. (47) are as follows: $\alpha=7.354\,12(-6)$, $\beta=8.9385(-6)$, $\gamma=0$. The evolution is shown in the nonrotating frame for one cycle of the microwave field. The initial wave packet of Eq. (47) was propagated in the rotating frame and the result was transformed to this frame. The propagation begins on the left-hand side at $t=0$ and scaled units are used throughout. The contours on the right-hand side show the zero-velocity surface (ZVS) halfway through the cycle. The grid is the same as used in Fig. 2. Note the resemblance to the Bohr atom.

and Fig. 3 confirms this expectation admirably: while in the rotating frame, the initial wave packet does nothing for 12 field cycles amounting to 107 ps, in the nonrotating frame itis revolving around the nucleus on a large circular orbit without spreading—much like a classical electron traveling on the circular orbits of the Bohr atom.

V. DISCUSSION AND CONCLUSIONS

The thesis of this and the previous article [19] can be summarized as follows: Coherent states of Rydberg atoms can be produced by a judicious combination of circularly polarized microwave and magnetic fields. The quantum mechanical simulations presented in this paper are the final confirmation of this thesis and corroborate earlier classical trajectory swarm results [19]. Our prescription is to expand the Hamiltonian in a Taylor series at a global equilibrium point: if the expansion is locally harmonic then a coherent state (defined by the local frequencies) will emerge (provided that the equilibrium point is linearly stable.) Such a coherent state (in the rotating frame) can neither spread nor disperse as it executes revolutions around the nucleus, although a Trojan wave packet will slowly decay due to tunneling. An additional, and, in general, more significant, source of dispersion, will arise if the tails of the wave packet penetrate appreciably into the nonlinear or chaotic parts of phase space [43]. This source of spreading can be anticipated by examining the contours of the ZVS, a classical-mechanical construct. In the laboratory frame, if these dispersive factors can be minimized, the electronic wave packet will travel along a circular Kepler orbit while remaining localized radially and angularly for a finite (but possibly very large) number of Kepler periods. An important point in our study is that the stability of such a packet can be enhanced considerably by using a magnetic field in addition to the CP field. Indeed, the initial wave packet and field choices displayed remarkable localization with the addition of a static magnetic field whereas the absence of this field can lead to rapid delocalization. Newly developed half-cycle pulses [62,63] show promise in the detection of these states.

But rising above mundane technical concerns for a moment, an exciting prospect emerges, and it is this: Schrödinger's motivation in those heroic days of quantum mechanics was not to invent yet another set of complicated quantum-mechanical wave packets but to create a classical electron in an atom. Our work, which produces wave packets that can be created and held together for experimentally feasible parameters, shows that physics is on the verge of realizing Schrödinger's dream.

ACKNOWLEDGMENTS

We thank Andrea Brunello for useful conversations. This work is performed under the auspices of the U.S. Department of Energy by the Lawrence Livermore National Laboratory under Contract No. W-7405-Eng-48. Partial support of this work by the American Chemical Society (Petroleum Research Fund) and the National Science Foundation is gratefully acknowledged.

[1] E. Schrödinger, Naturwissenschaften **14**, 664 (1926).
[2] E. Schrödinger, in Sources of Quantum Mechanics, edited by B. L. van der Waerden (Dover, New York, 1968).
[3] E. J. Heller, Phys. Rev. Lett. **53**, 1515 (1984).
[4] R. J. Glauber, Phys. Rev. **131**, 2766 (1963).
[5] E. Schrödinger, in Letters in Wave Mechanics, edited by K. Prizibram (Philos. Library, New York, 1967).
[6] L. S. Brown, Am. J. Phys. **41**, 525 (1973).
[7] J. Mostowski, Lett. Math. Phys. **2**, 1 (1977).
[8] D. Bhaumik, B. Dutta-Roy, and G. Ghosh, J. Phys. A **19**, 1355 (1986).
[9] C. C. Gerry, Phys. Rev. A **33**, 6 (1986).
[10] S. Nandi and C. S. Shastry, J. Phys. A **22**, 1005 (1989).
[11] M. Nauenberg, Phys. Rev. A **40**, 1133 (1989).
[12] J. C. Gay, D. Delande, and A. Bommier, Phys. Rev. A **39**, 6587 (1989).
[13] Z. D. Gaeta, and C. R. Stroud, Phys. Rev. A **42**, 6308 (1990).
[14] J. A. Yeazell and C. R. Stroud, Phys. Rev. A **43**, 5153 (1991).
[15] I. Zlatev, W-M. Zhang, and D. H. Feng, Phys. Rev. A **50**, R1973 (1994).
[16] M. Nauenberg, in *Coherent States: Past, Present and Future*, edited by D. H. Feng, J. R. Klauder, and M. R. Strayer (World Scientific, Singapore, 1994), p. 345.
[17] W.-M. Zhang, D. H. Feng, and R. Gilmore, Rev. Mod. Phys. **62**, 867 (1990).
[18] J. R. Klauder, J. Phys. A **29**, L293 (1996).
[19] E. Lee, A. F. Brunello, and David Farrelly, preceding paper Phys. Rev. A **55**, 2203 (1997).
[20] T. F. Gallagher, *Rydberg Atoms* (Cambridge University Press, Cambridge, 1994).
[21] J. A. Yeazell and C. R. Stroud, Phys. Rev. Lett. **60**, 1494 (1988).
[22] M. Mallalieu and C. R. Stroud, Phys. Rev. A **49**, 2329 (1994).
[23] J. A. Yeazell and C. R. Stroud, Phys. Rev. A **35**, 2806 (1987).
[24] Z. D. Gaeta, M. W. Noel, and C. R. Stroud, Phys. Rev. Lett. **73**, 636 (1994).
[25] J. A. Yeazell, M. Mallalieu, and C. R. Stroud, Phys. Rev. Lett. **64**, 2007 (1990).
[26] J. A. Yeazell, M. Mallalieu, J. Parker, and C. R. Stroud, Phys. Rev. A **40**, 5040 (1989).
[27] M. Nauenberg, C. Stroud, and J. A. Yeazell, Sci. Am. **270**, 44 (1994).
[28] R. J. Brecha, G. Raithel, C. Wagner, and H. Walther, Opt. Commun. **102**, 257 (1993); P. Nussenzveig, F. Bernardot, M. Brune, J. Hare, J. M. Raimond, S. Haroche, and W. Gavlik, Phys. Rev. A **48**, 3991 (1993).
[29] G. Alber and P. Zoller, Phys. Rep. **199**, 231 (1991).
[30] L. Marmet, H. Held, G. Raithel, J. A. Yeazell, and H. Walther, Phys. Rev. Lett. **72**, 3779 (1994).
[31] J. Wals *et al.*, Phys. Rev. Lett. **72**, 3783 (1994).
[32] C. Raman, C. W. S. Conover, C. I. Sukenik, and P. H. Bucksbaum, Phys. Rev. Lett. **76**, 2436 (1996).
[33] D. W. Schumaker, J. H. Hoogenraad, D. Pinkos, and P. H. Bucksbaum, Phys. Rev. A **52**, 4719 (1996).
[34] P. Fu, T. J. Scholz, J. M. Hettema, and T. F. Gallagher, Phys. Rev. Lett. **64**, 511 (1990).
[35] C. H. Cheng, C. Y. Lee, and T. F. Gallagher, Phys. Rev. Lett. **73**, 3078 (1994).
[36] M. Nauenberg, Phys. Rev. Lett. **64**, 2731 (1990).
[37] M. Nauenberg, Europhys. Lett. **13**, 611 (1990).
[38] P. Kappertz and M. Nauenberg, Phys. Rev. A **47**, 4749 (1993).
[39] V. Szebehely, *Theory of Orbits: The Restricted Problem of Three Bodies* (Academic, New York, 1967).
[40] D. Farrelly and T. Uzer, Phys. Rev. Lett. **74**, 1720 (1995).
[41] I. Bialynicki-Birula, M. Kaliński, and J. H. Eberly, Phys. Rev. Lett. **73**, 1777 (1994).
[42] D. Farrelly, E. Lee, and T. Uzer, Phys. Lett. A **204**, 359 (1995).
[43] D. Farrelly, E. Lee, and T. Uzer, Phys. Rev. Lett. **75**, 972 (1995).
[44] I. Bialynicki-Birula, M. Kaliński, and J. H. Eberly, Phys. Rev. Lett. **75**, 973 (1995).
[45] A. Buchleitner, thèse de doctorat, Université Pierre et Marie Curie, Paris, 1993 (unpublished).
[46] A. Buchleitner and D. Delande, Phys. Rev. Lett. **75**, 1487 (1995).
[47] J. Zakrzewski, D. Delande, and A. Buchleitner, Phys. Rev. Lett. **75**, 4015 (1995).
[48] D. Delande, J. Zakrzewski, and A. Buchleitner, Europhys. Lett. **32**, 107 (1995).
[49] E. Lee, A. F. Brunello, and D. Farrelly, Phys. Rev. Lett. **75**, 3641 (1995).
[50] A. F. Brunello, T. Uzer, and D. Farrelly, Phys. Rev. Lett. **76**, 2874 (1996).
[51] D. Apostolakis, E. G. Floratos, and N. D. Vlachos (unpublished).
[52] M. J. Rakovic, T. Uzer, and D. Farrelly (unpublished).
[53] A. Bohr and B. R. Mottelson, *Nuclear Structure Vol. II* (W. A. Benjamin, Reading, MA, 1975), pp. 84–88.
[54] K. F. Liu and G. Ripka, Nucl. Phys. **A293**, 333 (1977).
[55] D. Glas, U. Mosel, and P. G. Zint, Z. Phys. A **285**, 83 (1978).
[56] M. A. Z. Habeeb, J. Phys. G **13**, 651 (1987).
[57] A. Deprit, Astron. J. **71**, 77 (1966).
[58] A. Deprit and A. Deprit-Bartholomé, Astron. J. **72**, 173 (1966).
[59] A. Deprit in *The Big Bang and George Lemaitre*, edited by A. Berger (Reidel, Dordrecht, 1984), pp. 151–180.
[60] C. LeForestier *et al.*, J. Comput. Phys. **94**, 59 (1991).
[61] H. Goldstein, *Classical Mechanics* (Addison-Wesley, New York, 1950), pp. 69ff.
[62] R. R. Jones, D. You, and P. H. Bucksbaum, Phys. Rev. Lett. **70**, 1236 (1993).
[63] C. O. Reinhold, J. Burgdörfer, M. T. Frey, and F. B. Dunning, Phys. Rev. A **54**, R33 (1996).